

Barrel Distortion Correction with Estimation of Centre of Distortions and Focal Length for Fisheye Lenses

Guy Blanchard Ikokou
Tshwane University of Technology

Abstract:- With the mass production of non-metric cameras with unstable internal properties, the camera calibration task has become more and more sophisticated and difficult to perform. Several approaches are available in the literature with good performance. However, some of these techniques are laborious to perform and require the use of some distortion model specific algorithms, which cannot accommodate other types of models/lens distortion characteristics. Moreover, some of the proposed techniques require known coordinates of 3D points and can only handle small amounts of distortions. In this paper, we propose a new distortion correction model, which takes advantage of the properties of the hyperbolic curves and those of abstract geometry to estimate camera parameters without prior knowledge of the coordinates of the distortion center and 3D coordinates measures. Tested on an uneven building wall as calibration surface, the approach dealt with severe barrel distortion profile. The technique offers an analytical solution for the distortion coefficient in opposition to some of the existing approaches which suffers the limitations of iteration and Least Squares solutions which requires good initial estimates of the unknown parameters.

Keywords:- Fisheye Lenses, FOV Model, Barrel Distortions, Radial Distortions, Camera Calibration, Abstract Geometry.

I. INTRODUCTION

With the mass production of cheap lenses, non-metric cameras have been widely used for applications in fields such as Photogrammetry. Camera calibration is a very important task for applications in Photogrammetry, which requires accurate measurements. Methods of camera calibration have been proposed in the literature with various level of accuracies [Abdo and Borgeat, 2010]. For the most popular radial distortion model, the polynomial model is reported as not having an inverse model and its numerous terms make the analytical solutions very difficult to solve. The other limitation of the model is that it is not suitable for severe distortions [Orekhov et al., 2007; Aleman-Flores et al., 2013; Tang et al., 2017]. Some suggestions were made for the use of division models to handle complex distortions [Mei et al., 2015; Fitzgibbon, 2001]. Others have proposed rational models to correct lens distortions [Heikkila and

Silv, 1997]. Inverse models of the division and rational models have also been proposed in the literature but are reported unstable. Techniques which estimate the distortion parameters based on the line straightness constraint rely mostly on the extraction of curved lines from the imagery using curve fitting algorithms but the challenges with such methods is their sensitivity to image noise which can compromise the accuracy of the estimated parameters. Some of these algorithms are model specific and cannot perform efficiently with a different model/lens distortion characteristic. Furthermore, some cannot handle distortion profiles such as barrel and pincushion distortions at the same time due to their mathematical formulations. Other models have also been proposed to deal with more severe distortions (Aghayari et al., 2017; Hensel et al., 2018; Hsu et al., 2018). However, many of these models assume zero coordinates for the projection center. In this paper, we are proposing a radial distortion correction approach based on properties of hyperbolic curves and some analytical geometry principles to estimate the camera focal length and the coordinates of the distortion center as well as the distortion coefficient. The mathematical formulation of the model enables to estimate the camera parameters analytically. The model does not require the use of any optimization algorithm or knowledge of 3D points coordinates to correct image distortions.

II. RELATED WORK

Digital consumer grade digital cameras have been widely used in applications such as Photogrammetry. Several studies have reported measurement errors originating from the misalignment of optical systems [Wackow et al., 2007; Sanz-Ablanedo et al., 2009]. Camera calibration consist of estimating the camera intrinsic and extrinsic parameters [Tommaselli and Tozzi, 1999]. Line based approaches have been proposed to deal with the estimation of radial lens distortions and to address the limitations of points correspondence techniques which are highly error prone [Prescott and McLean, 1997]. The technique proposed in [Prescott and McLean, 1997] estimates distortion parameters based on geometric constraints of straight lines. The line extraction technique gathers pixels with similar texture properties based on their local gradient measures then uses the orientation gradient to refine their locations to form line support regions in order to generate straight lines [Burns et al., 1986]. The identified line support regions are used to estimate the parameters of

the distorted lines, which are then utilized in a wrapping function to produce the radial distortion coefficients as well as the coordinates of the distortion center using an optimization process. One limitation of the approach is its sensitivity to image noise, which could be mistakenly estimated as a line edge, and be incorrectly associated with the line's pixels. [Tommaselli and Tozzi] proposed a line based dynamic calibration technique based on the equivalent between an image line carried by the image plane and its corresponding carried by the 3D object plane. The line detection starts with setting gradient magnitude thresholds for each line edge. Pixels with gradient magnitude greater than the threshold are associated with the corresponding edge and all the pixels satisfying the threshold of a given edge are combined together to form a line [Dudani and Luk, 1978]. The line detection approach differs from that of [Burns et al., 1986] with the use of a Kalman filter to refine the point's coordinates on the distorted lines. A Least Squares Adjustment technique is used to fit the straight line to the identified edge points. One limitation of the approach is that distortion parameters are estimated following a batch procedure, which implies that any error with the initial values would propagate into the next output parameters. The other limitation of the approach is that the computation of the rotation matrix is not dissociated from the estimation of distortion parameters, resulting in residual propagation on the intrinsic parameters estimates. [Ahmed and Farag, 2005] proposed a line-based calibration procedure based on the line straightness. To quantify the distortions within the image the authors estimated an error measure from the slopes of the distorted curves and the straight line. To prevent the curve estimates from noise contamination the authors employed a Least-Median of Squares technique. [Song and Lee,2010/] proposed a five-step calibration approach, which first extracts curves in the image based on the pixel location and angular orientation with reference to candidate edge pixel. Once the curves are extracted from the image, the authors generated distortion parameters using Lavenberg-Marquardt algorithm, which are then used to correct the distorted curves, extracted in the initial phase of the calibration process. Although the technique produced promising distortion estimates, it requires good initial point's coordinates and any error in the curve extraction process may result in flawed location of the distortion center as well as other distortion parameters. [Thormaehlen and Wassermann, 2003] earlier proposed a calibration approach similar to [Song and Lee,2010] but instead of relying on pixel's coordinate their technique used distance thresholds to combine the different distorted curves to form straight lines and any curve segments located outside the distance threshold is not candidate for the merge. The approach also accounts for the line's angular orientation, as any deviation from the straight-line model should not exceed the set threshold in order for the pixel to be merged into the straight line. To estimate the distortion parameters from the polynomial model, the authors used a Random Sample Consensus technique [Fishler and Bolles, 2003]. The technique optimizes the parameters' estimates using Lavenberg Marquardt algorithm applied to a cost function.

III. MATERIAL AND METHODS METHODOLOGY

A. Lens and Processing Platforms

In this experiment, a wide-angle 235° field-of-view fisheye lens was used to capture three images of an uneven calibration surface of a three floor-building (Figure1). The three images were captured with varying camera orientation. The radially distorted image provides a full view of the calibration surface.



Fig 1 The Calibration Object Captured by a Fisheye Lens

From the calibration object were extracted 72 calibration points. The measurement of calibration points' coordinates was done using ArcGIS software package and the software choice was motivated by its user-friendly processing environment. The coordinates' computation and the testing of the model were all performed using MATLAB.

B. Description of the Projection Model

The proposed model is a hybrid model at the intersection of the spherical calibration methods and the line-based approaches. It consists of a distorted curve assimilated to a branch of a hyperbolic curve representing a line in the distorted image and a second "virtual" distorted curve that only serves for computation purposes. The choice of a hyperbolic curve was motivated by its approximation to a circular image produced by most of fisheye lenses. Both asymptotes of the curve intersect at a center $O(0,0)$ which is the origin of the semi axes as shown in Figure3.

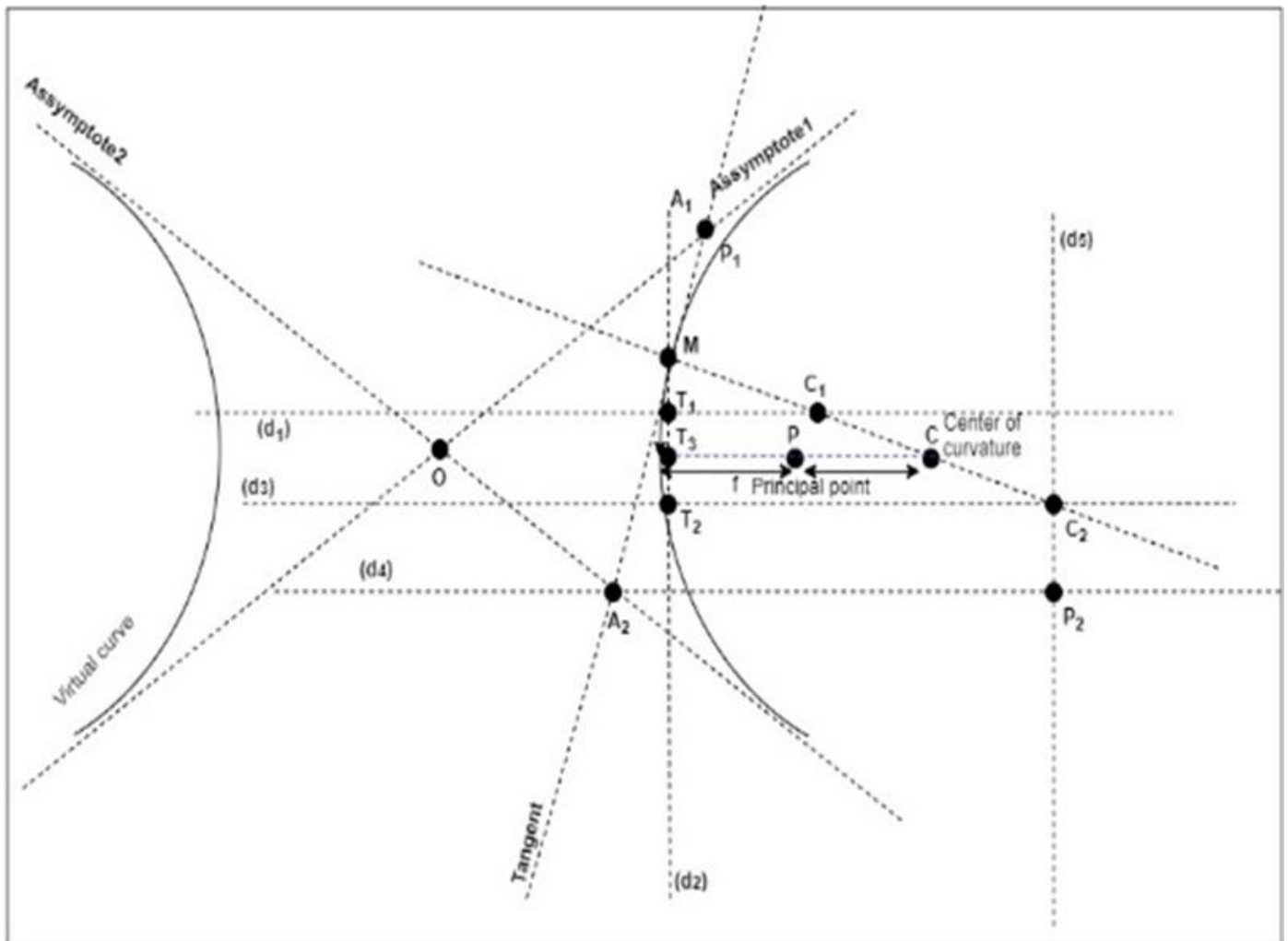


Fig 2 A Graphical Description of the Projection Model

To unpack the projection model, let C_1 and C_2 be two points on a diameter of the curvature of a distorted line such that the center of the circle at $C(x_c, y_c)$ is the symmetric center of $C_1(x_{c_1}, y_{c_1})$ and $C_2(x_{c_2}, y_{c_2})$. Let M be a distorted image point on the distorted curve such that $M \in (C_1C_2)$ and T be the tangent to the distorted curve at M with A_1, A_2 the intersection points of the tangent T with the asymptotes Π_1 and Π_2 of the curve. Let l_1 and l_2 be two lines passing through C_1, C_2 and perpendicular to the closest respective asymptote. This constraint guarantees that one of the intersection points P_1 or P_2 is either projected at A_1 or A_2 . From the property of the tangent to a circle, it results that:

$$(C_1C_2) \perp (A_1A_2) \tag{1}$$

To estimate the coordinates of the various intersection points it is important to note that from the polar equation of the hyperbola given by $x = a \sec \psi$, $y = b \tan \psi$ (2), the derivative of each coordinate function can be estimated with reference to ψ as follows:

$$\frac{dx}{d\psi} = a \tan \psi \sec \psi \text{ and } \frac{dy}{d\psi} = b \sec^2 \psi \tag{3}$$

Combining (2) into the standard equation of a hyperbola given by $\frac{x^2}{a^2} - \frac{y^2}{b^2} = 1$ (4), and after simplification, the equation of the tangent to the curve at any point M can be estimated as follows:

$$\frac{y \tan \psi}{b} - \frac{x \sec \psi}{a} = -1 \tag{5}$$

Similarly, the equation of the normal l_3 to the tangent at M and passing through C_1 and C_2 can be derived as follows:

$$\frac{yb}{\tan \psi} + \frac{ax}{\sec \psi} = a^2 + b^2 \tag{6}$$

Substituting (1) into (4) enabled to derive the polar equations of the asymptotes Π_1 and Π_2 to the curve as follows:

$$y = -\frac{x}{\cos \psi} \text{ And } y = \frac{x}{\cos \psi} \tag{7}$$

Intersecting the equations in (7) with the equation in (5) produces the coordinate estimates of A_1 and A_2 as follows:

$$A_2 = \left(\frac{ab \cos^2 \psi}{(b \cos \psi + a \sin \psi)}; \frac{ab \cos \psi}{(b \cos \psi + a \sin \psi)} \right)$$

and

$$A_2 = \left(\frac{b \cos \psi \times a \cos \psi}{(b \cos \psi - a \sin \psi)}; \frac{ab \cos \psi}{(b \cos \psi - a \sin \psi)} \right) \tag{8}$$

Since the line l_1 is perpendicular to Π_1 and intersect at A_1 its equation can be estimated as:

$$l_2 : y = x \cos \omega + b \tan \omega + a \tag{9}$$

With ω the polar coordinate of A_1 on the curve.

Intersecting l_2 with the normal l_3 gives the coordinate estimates of C_1 as follows:

$$x_{C_1} = \frac{a^2 \tan \psi + b^2 \tan \psi - b^2 \tan \omega - ab}{(a \sin \psi + b \cos \omega)} \tag{10}$$

$$y_{C_1} = \frac{\tan \psi \cos \omega (a^2 + b^2) + \sin \psi (ab \tan \omega + a^2)}{(a \sin \psi + b \cos \omega)}$$

Let (d_1) the horizontal line passing through C_1 and (d_2) the normal to (d_1) through M and that intersects with (d_1) at T_1 . Let (d_3) be the horizontal line passing through C_2 that intersects (d_2) at T_2 . The parallel (d_4) to (d_2) passing through A_2 intersects its normal (d_5) through C_2 at a point P_2 .

C. Estimating the Major and Minor Semi Axes of the Hyperbola

For geometric correctness, it is important to align the hyperbola's coordinate system with that of the camera. For the purpose, the rotation angles of the semi axes were extended to $2\pi \text{ rad}$ as illustrated in Figure4. The distance from the center of the hyperbola to that of the camera is now scaled by the factor b along the x axis. This will ensure that the computations are isolated from the distorted camera center as more weight is given to the center of the hyperbola.

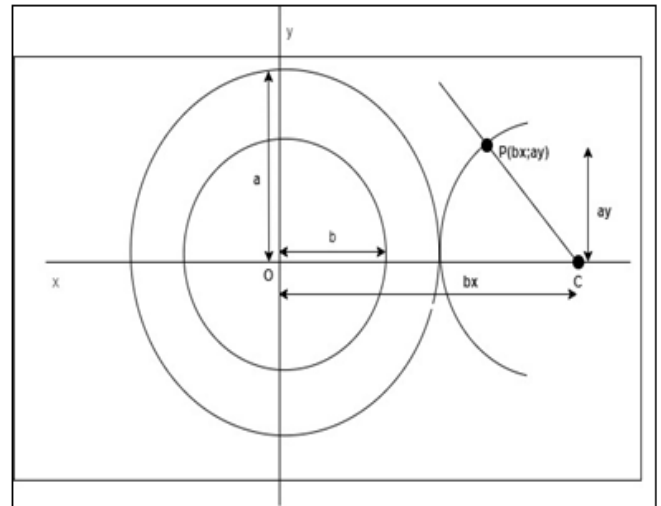


Fig 3 The Hyperbolic Fov Model.

Expanding the equation of the curve's asymptotes from the standard equation of the hyperbolic curve it is demonstrated that the semi-axes are estimated as follows:

$$a = \frac{y\sqrt{y^2 - 1}}{y^2 - 1} \tag{11}$$

$$\text{And } b = \frac{xy\sqrt{y^2 - 1}}{y^3 - y} \tag{12}$$

D. Estimating the Lens Focal Length

The general parametric equation of the radius of curvature of most conics is given as follows:

$$R = \frac{\left[(x'(t))^2 + (y'(t))^2 \right]^{3/2}}{(x')(y'') - (y')(x'')} \tag{13}$$

From the equations in (2), we can compute the first and second derivatives for each parametric variable as follows:

$$x' = \frac{-a \sin \theta}{(\cos \theta)^2} \quad x'' = \frac{a(\cos \theta)^2 - 2a(\sin \theta)^2}{(\cos \theta)^3} \tag{14}$$

$$y' = \frac{b}{(\cos \theta)^2} \quad y'' = \frac{-2b[(\sin \theta)]}{(\cos \theta)^3} \tag{15}$$

Combining equations in (14) and (15) into (13) gives:

$$R = \frac{a^3 \left[\frac{-(\cos \theta)^2 + \frac{a^2 + b^2}{a^2}}{(\cos \theta)^4} \right]^{\frac{3}{2}}}{\frac{ab}{(\cos \theta)^3} = \left(\frac{b}{(\cos \theta)^2} \right) \left(\frac{a(\cos \theta)^2 - 2a(\sin \theta)^2}{(\cos \theta)^3} \right)} \tag{16}$$

$$R = \frac{a^2 \left[\left(\frac{a^2 + b^2}{a^2} \right) - (\cos \theta)^2 \right]^{\frac{3}{2}}}{b(\cos \theta)^3} \tag{17}$$

From the property of the spherical lenses, we have:

$$f = \frac{a^2 \left[\left(\frac{a^2 + b^2}{a^2} \right) - (\cos \theta)^2 \right]^{\frac{3}{2}}}{2b(\cos \theta)^3} \tag{18}$$

E. Distortion Center Estimation

The underlying hypothesis to the proposed model is that there exists an infinity of symmetric points p_{i-1} and p_{i+1} with reference to the center $C(x_c, y_c)$ of a circle along its diameter and satisfying the equation:

$$x_c = \frac{x_{i-1} + x_{i+1}}{2} \quad \text{and} \quad y_c = \frac{y_{i-1} + y_{i+1}}{2} \tag{19}$$

Finding any of these couples of points satisfying the equations (19) enables to estimate the coordinates of the center C . From Figure2, the length of the segment $[A_2C_2]$ can be estimated using the Pythagoras theorem as follows:

$$A_2C_2 = \sqrt{(MA_2)^2 + (MC_2)^2} \tag{20}$$

In the triangle $\Delta A_2C_2P_2$ let β be the angle at A_2 . It can be demonstrated that the distance d_1 from P_2 to C_2 can be estimated as follows:

$$d_1 = A_2C_2 \cos \beta \tag{21}$$

Thus, giving the y coordinate of C_2 as follows:

$$y_{C_2} = y_{A_2} + d_1 \tag{22}$$

Similarly let d_2 be the horizontal distance from A_2 to C_2 , the x coordinate of C_2 is given by:

$$x_{C_2} = x_{A_2} + A_2C_2 \sin \beta \tag{23}$$

Let κ be the angle at C_2 in the triangle A_2MC_2 . It can be demonstrated that:

$$\tan \kappa = \frac{A_2M}{MC_2} \tag{24}$$

With the distance MC_2 equal to twice the focal length. Let α be the angle at C_2 in the triangle ΔMT_2C_2 . Furthermore, in the triangle ΔMC_1T_1 the angle ϕ at C_1 can be estimated knowing any of the distances T_1C_1 or T_1M considering that $T_1C_1 = x_{C_1} - x_M$ and $T_1M = y_M - y_{C_1}$. From the corresponding-angles, property in the triangles ΔMC_1T_1 and ΔMT_2C_2 it can be proven that:

$$\phi = \alpha \quad \text{then} \quad \beta = 90 - \phi \tag{25}$$

With $\phi = \kappa - \alpha$.

Furthermore, it can be observed in Figure3 that in the right-angle triangle ΔMT_3C that:

$$T_3M = \sqrt{(x_M - x_{T_3})^2 + (y_M - y_{T_3})^2} \tag{26}$$

$$\sin \alpha = \frac{MT_3}{MC} \tag{27}$$

From (26) it can be observed that:

$$y_{T_3} = y_M - MC \sin \alpha \tag{28}$$

Substituting (28) enables to estimate x_{T_3} .

It can also be observed that

$$PT_3 = \sqrt{(x_{T_3} - x_P)^2 + (y_{T_3} - y_P)^2} \tag{29}$$

$$\text{And } CP = \sqrt{(x_P - x_C)^2 + (y_P - y_C)^2} \tag{30}$$

IV. RESULTS

The table 2 shows a summary of the calibration results in millimeter. The first two columns of the table show the calibrated values of the semi major axis a and the semi minor axis b . An analysis of the estimates reveals that there seems to be a correlation between the semi major axis of the hyperbola and the estimate of the focal length of its assimilated lens. The two high estimates of the major semi axis with the first and third image resulted in the two high estimates of the focal length.

Table 2 Presentation of Some Calibration Results.

	a	b	f	x_p	y_p
Image1	4.83	3.21	16.353	0.0212	0.084
Image2	2.14	5.42	15.985	0.214	0.092
Image3	5.36	2.72	16.25	0.018	0.099
Image4	2.63	5.84	15.54	0.039	0.078

The average focal length values were found ranging between 15 and 16 for the second and four images while slightly above 16mm for the first and third image. This may be due to the fact that the first and third image were captured with greater angles from the vertical in comparison with the second and four images. The deviations from the mean for the x and y coordinates of the projection center were found very negligible. Moreover, the third image produced the highest distortion coefficient probably associated with the high estimate of the y coordinate of the projection center. It could be assumed that errors in the estimate of the y coordinate can affect the performance of the distortion coefficient value. The figure6 shows the distorted images.

V. CONCLUSION

Properties of hyperbolic functions and abstract geometry have widely been used in other engineering and science fields such as Physics but their contributions in Photogrammetry remains very limited. The study proposed a new calibration approach relying on some properties of hyperbolic curves and abstract geometry to deal with barrel distortions produced by fisheye lenses for applications requiring large view of the scene. The approach produced estimates of focal lengths, which are descriptive of a full frame fisheye lens (Alessandri et al., 2019). The approach enables the estimation of the distortion center from simple geometric projection properties. Among the advantage of the proposed approach is the non-assumption of coordinates of the projection center to be at (0, 0) in contrast to the approach proposed in Park et al., (2014). Our proposed undistorted radius is estimated from the origin of the hyperbolic coordinate system to prevent any instabilities that could originate from the camera projection center. The straightforward and non-requirement for a least Squares Solution are also added advantages of the proposed technique as the Least Squares Solutions tend to over fit the data when the model is over-parameterized and also requires initial parameter estimates which may be an issue. No 3D point coordinates are needed to compute camera parameters and no iteration is required for the optimization of the distortion coefficient because the approach analytically estimates the root solutions that minimize the distance error between the distorted point and its undistorted location. The scaling process of coordinates by the semi axes factors also offers an advantage of minimizing the influence residuals from the projection center on the estimated parameters. This study will be extended to the corrections of barrel distortions from UAV imagery. In a further testing of the technique more points will be collected around the edge of the imagery to evaluate performance improvements.



Fig 5 Visual Results of Distortion Corrections

The image shows that the barrel distortions have largely been dealt with. The top part of the building has been straightened although there are slight visible artifacts still remaining on the corrected image. This could be explained by the fact that the correction procedure is a localized approach and rely mostly on the extracted coordinates of points and the distortion magnitude was more severe when moving away from the image center.

REFERENCES

- [1]. Abdo N. and A. Borgeat, A., 3D camera calibration. Technical report, 2010
- [2]. Aghayari, S., Saadatseresht, M., Omidalizandi, M. and Neumann, I., 2017. Geometric calibration of full spherical panoramic Ricoh-Theta camera. *ISPRS Annals of the Photogrammetry, Remote Sensing and Spatial Information Sciences IV-1/W1* (2017), 4, pp.237-245.
- [3]. Ahmed M., and Farag, A., "Nonmetric calibration of camera lens distortion: differential methods and robust estimation", *IP* (14) 8, 1215–1230 (2005).
- [4]. Alemán-Flores, M., Alvarez, L., Gomez, L. and Santana-Cedrés, D., 2013, November. Wide-angle lens distortion correction using division models. In *Iberoamerican Congress on Pattern Recognition* (pp. 415-422). Springer, Berlin, Heidelberg.
- [5]. Alessandri, L., Baiocchi, V., Del Pizzo, S., Rolfo, M.F. and Troisi, S., 2019. Photogrammetric Survey with Fisheye Lens for the characterization of the La Sassa Cave. *International Archives of the Photogrammetry, Remote Sensing & Spatial Information Sciences*.
- [6]. Burns, J.B., Hanson A.R., and Riseman, E.M., "Extracting Straight Lines," *IEEE Trans. Pattern Analysis and Machine Intelligence*, vol. 8, no. 4, pp. 425-455, July 1986.
- [7]. Dudani S.A., and Luk, A.L., "Locating straight line edge segments on outdoor scenes," *Patterni Recog.*, vol. 10, no. 3, pp. 145-166, 1978.
- [8]. Fischler M.A. and Bolles, R.C., "Random sample consensus: a paradigm for model fitting with applications to image analysis and automated cartography". *Communications of the ACM*, 24(6), 1981, pp.381-395.
- [9]. Fitzgibbon, A.W., "Simultaneous linear estimation of multiple view geometry and lens distortion". In: *Proc. IEEE International Conference on Computer Vision and Pattern Recognition* pp. 125–132 (2001)
- [10]. Heikkil J., and Silvén, O., "A four-step camera calibration procedure with implicit image correction," in *IEEE Computer Society Conference on Computer Vision and Pattern Recognition*, San Juan, Puerto Rico, 1997, pp. 1106–1112. Prescott B and McLean, F.F., "Line-based correction of radial lens distortion" *Graphical Models and Image Processing*, 1997, 59(1), pp.39-47.
- [11]. Hensel, S., Marinov, M.B. and Schwarz, R., 2018, September. Fisheye camera calibration and distortion correction for ground-based sky imagery. In *2018 IEEE XXVII International Scientific Conference Electronics-ET* (pp. 1-4). IEEE.
- [12]. Hsu, C.Y., Chang, C.M., Kang, L.W.K., Fu, R.H., Chen, D.Y. and Weng, M.F., 2018, May. Fish-Eye Lenses-Based Camera Calibration and Panoramic Image Stitching. In *2018 IEEE International Conference on Consumer Electronics-Taiwan (ICCE-TW)* (pp. 1-2). IEEE.
- [13]. Mei, X., Yang, S Rong, J., Ying, X., Huang S and Zha, H., 2015, September. Radial lens distortion correction using cascaded one-parameter division model. In *Image Processing (ICIP), 2015 IEEE International Conference*, 2015, (pp. 3615-3619).
- [14]. Orekhov, V., Abidi, B., Broaddus and M. Abidi, C., "Universal camera calibration with automatic distortion model selection," in *Proceedings of International Conference on Image Processing (IEEE, 2007)*, pp. 397–400.
- [15]. Park, D.H., Seo, J.G., Choi, H. and Kang, E.S., 2014. Distortion Center Estimation Technique Using the Fov Model and 2D Patterns. In *Proceedings of the International Conference on Image Processing, Computer Vision, and Pattern Recognition (IPCV)* (p. 1). The Steering Committee of the World Congress in Computer Science, Computer Engineering and Applied Computing (WorldComp).
- [16]. Song G.Y. and Lee, J.W., "Correction of radial distortion based on line-fitting", *Int. J. Control, Autom. Syst.* 8(3), 615–621 (2010).
- [17]. Sanz-Ablanedo, E., Rodríguez-Pérez J.R. and Arias-Sánchez, R., "Metric potential of a 3D measurement system based on digital compact cameras", *Sensors*, 2009; 9: 4178–4194.
- [18]. Tang, Z., von Gioi, R.G, Monasse P. and Morel, J.M. "A precision analysis of camera distortion models," *IEEE Trans. Image Process.*, vol. 26, no. 6, pp. 2694–2704, Jun. 2017.
- [19]. Thormaehlen H.B. and Wassermann, I "Robust line-based calibration of lens distortion from a single view". In *Mirage 2003*, pages 105-112, 2003.
- [20]. Tommaselli A.M.G. and Tozzi, C.L. "Line based camera calibration in machine vision dynamic applications". *Controle and Automacao*. 1999.
- [21]. Wackrow, R., Chandler, J, H., and Bryan, P., "Geometric consistency and stability of consumer-grade digital cameras for accurate spatial measurement". *Photogrammetric Record*, 2007, 22(118): 121–134.
- [22]. Wang, A. Qiu, T. and L. Shao, "A simple method of radial distortion correction with centre of distortion estimation," *Journal of Mathematic Imaging and Vision*, vol. 35, no. 3, pp. 165-172 Nov. 2009.